

Molten fluorides for nuclear applications

The importance of pyrochemistry is being increasingly acknowledged and becomes unavoidable in the nuclear field. Molten salts may be used for fuel processing and spent fuel recycling, for heat transfer, as a homogeneous fuel and as a breeder material in fusion systems. Fluorides that are stable at high temperature and under high neutron flux are especially promising. Analysis of several field cases reveals that corrosion in molten fluorides is essentially due to the oxidation of metals by uranium fluoride and/or oxidizing impurities. The thermodynamics of this process are discussed with an emphasis on understanding the mass transfer in the systems, selecting appropriate metallic materials and designing effective purification methods.

Sylvie. Delpech^{a*}, Céline Cabet^b, Cyrine Slim^a, Gérard S. Picard^a

a LECIME, Laboratoire d'Electrochimie, de Chimie des Interfaces et de Modélisation pour l'Energie, CNRS-UMR7575 - ENSCP - 11 rue Pierre et Marie Curie, 75231 PARIS CEDEX 05, France

b CEA, DEN, DPC, SCCME, Laboratoire d'Etude de la Corrosion Non Aqueuse, F-91191 Gif-sur-Yvette, France

*E-mail: sylvie-delpech@chimie-paristech.fr

High temperature molten salts based on chloride or fluoride compounds have several applications in the nuclear field. In the front-end nuclear fuel cycle, molten salts are used for the purification and production of zirconium alloy, which is used as fuel cladding. Then, a pyrochemical treatment in NaCl-AlCl₃ molten salt at 350 °C enables the separation of zirconium and hafnium, which is a neutronic poison¹. In the nuclear fuel fabrication process, conversion of uranium oxide ore requires large quantities of fluorine that is obtained by the electrolysis of 2HF-KF molten salt at 95 °C². Several pyrochemical processes based on chloride or fluoride molten salts have also been conceived in the back-end nuclear fuel cycle, to separate actinides from lanthanides

during nuclear waste recycling³⁻⁹. Because fluoride mixtures are thermodynamically stable at high temperature, with very high boiling points, these liquids have been considered as heat transfer or cooling fluids, as coolants for thermal energy^{10,11} and in nuclear fission and fusion systems. Several criteria have to be considered when choosing a structural material: mechanical strength at high temperature, irradiation resistance (in the case of materials under neutron flux) and chemical corrosion resistance (which depends on the material composition and microstructure, and on the physical chemistry of the molten salt). As it will be shown, in order to avoid corrosion the liquid fluoride salt coolant must be thermodynamically stable relative to the chosen materials.

If molten salts are already industrially used in the front-end nuclear fuel cycle or considered for alternative nuclear spent fuel recycling in the back-end fuel cycle, then the material development and the corrosion studies are essentially performed within the frame of the development of future nuclear reactors: Molten Salt Reactors (MSR), Advanced High Temperature Reactors (AHTR) and Tokamak fusion power plants. For all these cases, the selected molten salt is a fluoride salt mixture. Indeed, the material resistance is a key issue in all applications, but especially so in the case of reactor core use; not only because of the irradiation damage, but also because the operating temperature is determined by the fission reaction and cannot be decreased easily e.g. in case of pit formation. In the other applications the reactor can be cooled more easily.

The purpose of this paper is to give several causes of the chemical corrosion of materials in a fluoride salt and to propose, using a thermodynamical approach, some ways to prevent and control the chemical corrosion.

Description of the material/salt systems

Several fluoride molten salts have been investigated for nuclear applications:

- (a) LiF-BeF₂ (66-33mol%) (FLiBe) was extensively studied in the 60s at Oak Ridge National Laboratory (USA) for the development of thermal neutron spectrum molten salt reactor systems (MSRE for Molten Salt Reactor Experiment and MSBR for Molten Salt Breeder Reactor)¹²⁻¹⁵. In these designs the main in-core material was graphite, and a Ni-based alloy (Hastelloy-N) was used for the out-of-core structures. The problems associated with graphite use are its low life time under irradiation (5 years)¹⁶, a lack of recycling processes and no waste management.
- (b) LiF-BeF₂ salt is also a candidate for blanket coolants in fusion nuclear power plants. Indeed, tritium can be produced by neutronic reaction with lithium¹⁷⁻¹⁹ and using LiF salt instead of metallic Li (which is highly reactive with water and oxygen) is more secure. Moreover FLiBe salt has a low tritium solubility and therefore low tritium inventory¹⁸. Several corrosion studies of structural materials have been performed for this application²⁰⁻³⁰.
- (c) The AHTR (Advanced High Temperature Reactor) concept is currently studied in the nuclear fission field. This concept includes a solid fuel and a solid core associated with a molten salt as coolant. Due to its high thermal stability (the reactor operating temperature is greater than 900°C), the selected salts for primary and secondary coolants are LiF-BeF₂ (66-34 mol%) and LiF-NaF-KF (46.5-11.5-42 mol%) (FLiNaK)³¹⁻³³. From a neutronic point of view, the use of LiF-BeF₂ is recommended for the primary coolant.
- (d) Since 2000, an innovative design of MSR, the Molten Salt Fast Reactor (MSFR) has been studied by CNRS-France³⁴⁻³⁸. The liquid fuel considered in this concept is LiF-ThF₄-UF₄ (77-20-3 mol%).

Compared to the American MSRE and MSBR concepts, the MSFR operates with a fast neutronic spectrum. Under these conditions, the operating temperature of the reactor ranges between 650 and 850 °C, possibly higher than in the past American MSR systems. In this design, graphite is replaced by a metallic alloy.

In all these nuclear applications, the chemical resistance to the fluoride salts at high temperature is a key element in the choice of structural material. In the case of applications (b) and (d), the neutronic irradiation resistance must also be considered.

For the AHTR reactor system³³, several alloys were studied by immersing metallic samples in static FLiNaK salt at 850 °C for 500 hours: Haynes-230, Inconel-617, Hastelloy-N, Hastelloy-X, Nb-1Zr, Incoloy-800H, Ni-201 (nearly pure Ni). For the four Ni-based alloys considered, Hastelloy-N, Hastelloy-X, Inconel-617 and Haynes-230, the weight loss due to corrosion was found to increase with the Cr-content of the alloy. For Haynes-230, the significant chromium loss triggered dissolution/precipitation phenomena, especially the formation of W-rich precipitates at grain boundaries. The refractory alloy Nb-1Zr exhibited severe corrosion and embrittlement. Due to the remarkably high corrosion resistance of Ni in molten fluoride salts, Ni-201, a predominantly Ni-containing alloy with no Cr, was virtually immune to attack.

Concerning fusion applications²⁰⁻³⁰, the material should be chemically compatible with FLiBe, resistant to radiation damage and have inherently low activation to avoid excessive waste management at the end of plant life. No currently available material can meet all these requirements. From the stand point of corrosion resistance at high temperature, Ni-based alloys are the most resistant structural material to the fluoride salts. That is due to both the high value of the redox system NiF₂/Ni and the low solubility of NiF₂ in FLiBe salt³⁹. Nevertheless, high-nickel alloys are highly sensitive to neutron radiation damage and the activation products are longer-lived radioisotopes. The operating temperature of a fusion plant is lower than 650 °C and the chemical corrosion of steels and other metallic materials which meet low activation criteria may be slow enough at this temperature. Fe and V-based alloys containing Cr have been investigated in various molten salts^{20,21,27,29}. 304 and 316 stainless steels were down-selected^{17,18,24}. Reactions in the fusion blanket lead to formation of tritium (T), for which the oxidation state depends on the melt redox potential: T(+I)F or T₂(⁰).

Many papers describe material development for nuclear reactor applications⁴⁰⁻⁴⁹. Graphite presents an excellent compatibility with molten fluorides but cannot be used for structural applications. After preliminary tests, Cu, Mo, Nb, Ni and austenitic alloys were considered good candidates. However, Cu possesses insufficient mechanical resistance at high temperatures, and the forming of high Mo and Nb-alloys is complex. Corrosion tests have shown that Ni-based alloys were more resistant against chemical corrosion than the austenitic stainless alloys. For these two types of material, the chemical corrosion increases with the Cr content. Intensive corrosion of Inconel-600 was

observed with void formation in the bulk due to the selective dissolution of Cr. The corrosion resistance of Hastelloy-B, without any Cr, is excellent, but it was ruled out due to inadequate forming possibilities⁴⁶ and poor oxidation resistance in air. Decreasing the amount of Mo helps for forming and machining, and adding a small quantity of Cr limits air oxidation. An optimum Cr content of 6 to 8wt% was retained. Chemical composition of the MSRE structural alloy, Inor 8 or Hastelloy-N, followed these specifications. The dissolution rate of this alloy in fluoride molten salt at 700 °C was observed to be lower than 2.5 µm/year. However, experience from the MSRE has found that Ni-based alloys are embrittled under neutronic irradiation. Helium is produced (essentially) by the nuclear reaction, $^{58}\text{Ni} (n, \alpha) ^{55}\text{Fe}$, and nucleated as discrete voids within the alloy matrix. Nb and Ti are added into the metallic alloy to form intergranular carbides which are likely to trap helium atoms and prevent their diffusion along grain boundaries. The quantities of Ti and Nb should remain small to prevent the formation of $\text{Ni}_3(\text{Ti}, \text{Nb})$ phases. The carbides stability depends on the temperature: at 650 °C, 0.5% Ti+Nb is sufficient while at 700 °C, 2% is necessary⁴⁶.

Alloys strengthened by the addition of tungsten, to replace molybdenum, are under development^{38,50}. These alloys boast an increased mechanical resistance at high temperature, as previously described³⁸, while keeping the appropriate compatibility with molten fluorides. Hence such materials may allow higher operating temperatures (above 850 °C). Fabrication and analysis of W-rich alloys are ongoing in the frame of the European research project EVOL (EURATOM-FP7). Moreover, and as will be observed in the following, tungsten presents a higher chemical resistance against corrosion than molybdenum.

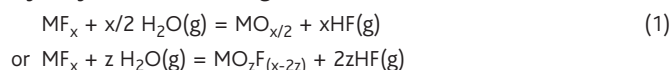
Main causes of chemical corrosion in fluoride molten salts

The chemical corrosion^{41,42,51} is due to the oxidation of a metal or an alloy in contact with its environment. Fig. 1 presents a schematic of the interface between the reacting element from the structural material and the molten salt medium.

The oxidizing species contained in the initial melt

In a fluoride melt, the main oxidizing impurities are said to be H_2O (in general this is present in the solid constituents to be fused) and HF (formed in the melt by several reactions):

Hydrolysis reaction during melt fusion:



The hydrolysis temperature (given for a Gibbs energy equal to 0 for Eq. 1) of selected pure salts was calculated from the thermochemical data of pure compounds⁵² (Table 1). Generally, the salt mixture is fused at a lower temperature than the hydrolysis temperature of the pure salt. Therefore, the solvation process increases the metallic

Table 1 Pure compounds hydrolysis temperature corresponding to an equilibrium constant (R1) of 1

| Reaction | T (°C) |
|---|--------|
| $\text{BeF}_2 + \text{H}_2\text{O}(\text{g}) = \text{BeO} + 2\text{HF}(\text{g})$ | 700 |
| $\text{ThF}_4 + 2\text{H}_2\text{O}(\text{g}) = \text{ThO}_2 + 4\text{HF}(\text{g})$ | 850 |
| $\text{ThF}_4 + \text{H}_2\text{O}(\text{g}) = \text{ThOF}_2 + 2\text{HF}(\text{g})$ | 840 |
| $\text{ZrF}_4 + 2\text{H}_2\text{O}(\text{g}) = \text{ZrO}_2 + 4\text{HF}(\text{g})$ | 495 |
| $\text{UF}_4 + 2\text{H}_2\text{O}(\text{g}) = \text{UO}_2 + 4\text{HF}(\text{g})$ | 660 |
| $\text{UF}_4 + \text{H}_2\text{O}(\text{g}) = \text{UOF}_2 + 2\text{HF}(\text{g})$ | 680 |
| $2\text{LiF} + \text{H}_2\text{O}(\text{g}) = \text{Li}_2\text{O} + 2\text{HF}(\text{g})$ | 3320 |
| $2\text{NaF} + \text{H}_2\text{O}(\text{g}) = \text{Na}_2\text{O} + 2\text{HF}(\text{g})$ | 3300 |
| $2\text{KF} + \text{H}_2\text{O}(\text{g}) = \text{K}_2\text{O} + 2\text{HF}(\text{g})$ | 4200 |

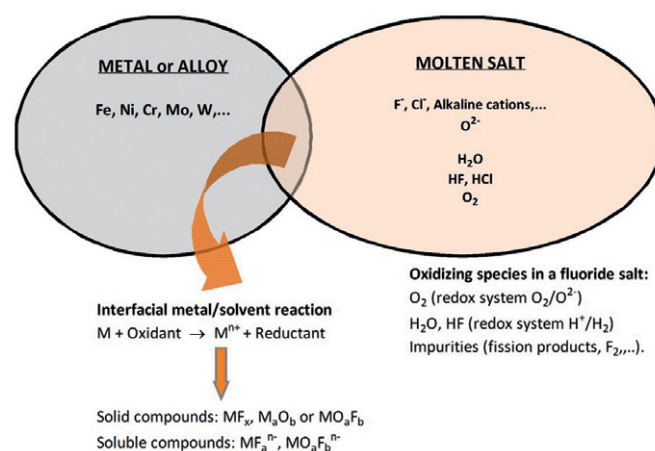


Fig. 1 Scheme of the metal/salt interface reactions.

fluoride stability and strongly reduces its hydrolysis process (less than 10 ppm for FLiNaK)^{29,30}.

Dissolution of water

$\text{H}_2\text{O}(\text{g})$ is easily eliminated under argon flux at temperatures above 300 °C. Moreover, traces of water are not stable in the fluoride salt after melting, as the water reacts with the fluoride ions to produce HF(g) and oxides.

Melt purification towards oxides

Although oxide ions^{53,54} have no direct influence on the structural material corrosion, because O^{2-} is not oxidizing towards metals, the elimination of oxides is nevertheless required to prevent the precipitation of metallic oxides (especially UO_2). O^{2-} ions react with an excess of HF according to the reaction:



It was suggested that this purification could be performed by bubbling pure gaseous HF or HF/ H_2 mixtures into the salt. Due to its high solubility in the fluoride salts, HF(g) is strongly retained in the salt^{55,56} and is responsible

for structural material corrosion as observed in corrosion tests^{20-23,25-30}. Therefore, the use of pure HF(g) is not recommended for salt purification because it will result in the severe corrosion of the structural material. This corrosion could be reduced by using a mixture of HF(g)/H₂(g), because the presence of H₂(g) will decrease the redox potential of the salt, and the H₂(g) can react with the oxidizing impurities of the salt.

Nevertheless, a purification procedure of molten salt with no introduction of pure HF(g) is strongly recommended to prevent corrosion reactions. The fluoride mixture could be dried under high vacuum prior to melting. It was observed that after a vacuum treatment (10⁻⁵ torr) at 400–425°C the cathodic and anodic residual currents (due to O²⁻ oxidation or HF-H₂O reduction) were smaller than those measured by other authors in the same melt pretreated with HF and H₂^{42,57,58}. The elimination and purification of salts for removing oxides and sulfurs can also be performed by gas mixture bubbling. In this case the HF/H₂ gas composition has to be carefully chosen to prevent an excess of HF and an increase of salt redox potential.

The oxidizing species related to the fission reaction

In the case of MSR, the molten salt chemical composition varies with the fission reaction and therefore with the operating time. In particular, it was assessed that the redox potential of the fuel salt will increase while in service. The fissile element in the MSFR reactor system is ²³³U which is present with two oxidation states in the salt, (IV) and (III), as UF₄ and UF₃ respectively. Then, the redox potential of the fuel salt depends on the x(UF₄)/x(UF₃) mole fraction ratio according to the Nernst relation:

$$E_{\text{fuel salt}} = E^{\circ}_{\text{UF}_4/\text{UF}_3} + \frac{2.3RT}{F} \log \frac{x(\text{UF}_4)}{x(\text{UF}_3)} \quad (3)$$

where R is the ideal gas constant (J/mol/K), F the Faraday constant (C), T the temperature (K) and E^o the apparent potential of the UF₄/UF₃ redox system which combines the standard potential of UF₄/UF₃ and the activity coefficients of UF₄ and UF₃.

When the fission reactions occur, the fission products are essentially LnF₃ lanthanides (with oxidation state (III)) and gaseous products or noble metals (M) (with oxidation state 0). The result of the fission reactions on the salt chemistry can be schematized by³⁸:



When the fission reaction (Eq. 5) occurs, gaseous fluorine is produced. Fluorine being the most oxidizing species, the salt redox potential increases according to:



Consumption of UF₃ by Eq. 4 and Eq. 6 leads to an increase of the redox potential according to Eq. 3. **The fluorine production, and**

consequently the fuel potential, strongly enhances the corrosion of the structural materials during the reactor's operating time. As it will be shown below, addition of a reducing agent is required to curb the increase of the salt potential and thus to limit corrosion.

Some fission products such as S, Se and Te are also harmful to the metallic structures due to their oxidizing properties; specifically, due to their negative oxidation states ((-I) and (-II)). In particular, corrosion tests have shown that a low concentration of metallic tellurium is strongly corrosive and causes intergranular attacks on Ni-alloys resulting in severe embrittlement^{13,47,59} (Fig. 2). Analysis of stability phase diagrams calculated for tellurium in fluoride salts, combined with experimental results, showed that the deleterious effect of Te can be cancelled by applying a cathodic polarization to the material⁶⁰. In this case, tellurium, electrochemically reduced to Te(-II), reacts with ZrF₄ (salt constituent) to form ZrTe₂.

The oxidation state of the fission products (Te for example) depends on the salt redox potential at the time of its formation. For high values of the salt potential, Te should be in metallic form and could react with the structural material according to:



The tellurium is thought to be responsible for the formation of brittle telluride compounds at the alloy grain boundaries. For low salt potentials, tellurium is produced in a Te(-II) state and combines with metallic salt cations (as oxide ions behave).

Thermal gradient and mass transfer

A main cause of sustained corrosion in MSR is the existence of thermal gradients within the molten fuel salt, which may be responsible for mass transfer⁴². This was experimentally demonstrated by Koger using thermal convection loops; it was observed that adding an oxidizing agent to a molten salt increases the overall corrosion rate^{61,62}.

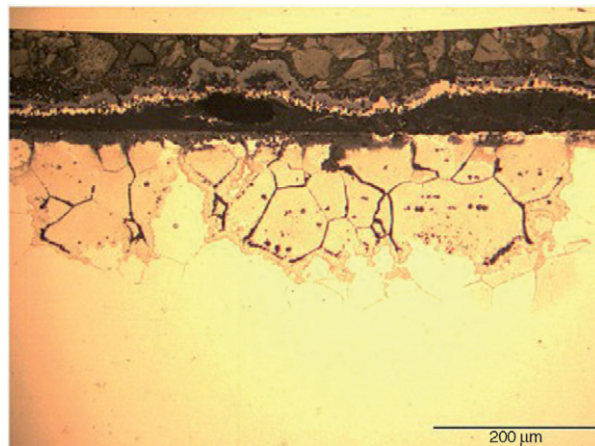
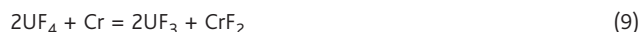


Fig. 2 Intergranular attack of Ni-based alloy (56.5Ni - 21.5Cr - 13.7Mo - 3.8Fe - 3W) by metallic Te in fluoride salt at 700 °C.

The oxidation of Cr (the most reactive metal in structural materials) depends on the salt potential and therefore on the mole fraction ratio $x(\text{UF}_4)/x(\text{UF}_3)$ (Eq. 3). This can be written according to the equilibrium equation:



The experimental constant K_N is defined by:

$$K_N = \frac{x(\text{CrF}_2)x(\text{UF}_3)^2}{x(\text{Cr})x(\text{UF}_4)^2} \quad (10)$$

This constant is calculated from experimental measurements of LiF-BeF₂ molten salt in contact with Hastelloy-N for various ratios of UF_4/UF_3 . This constant is related to the mole fraction of the compounds, and the activity coefficients are included within the constant. This relation correlates the mole fraction of dissolved chromium $x(\text{CrF}_2)$ and the salt redox potential (given by the ratio UF_4/UF_3); Grimes⁶³ assumed that the activity of Cr is equal to its mole fraction in the alloy ($x(\text{Cr})=0.083$):

$$x(\text{CrF}_2) = K_N x(\text{Cr}) \frac{x(\text{UF}_4)^2}{x(\text{UF}_3)^2} \quad (11)$$

The constant K_N has been experimentally determined as a function of the temperature⁶⁴:

$$\ln(K_N) = (-183910.87 + 57.63T)/(RT) \quad (12)$$

The variation of the mole fraction of dissolved CrF_2 with temperature has been calculated from Eq. 11 for two different values of salt redox potential (Fig. 3). This change in the equilibrium mole fraction of

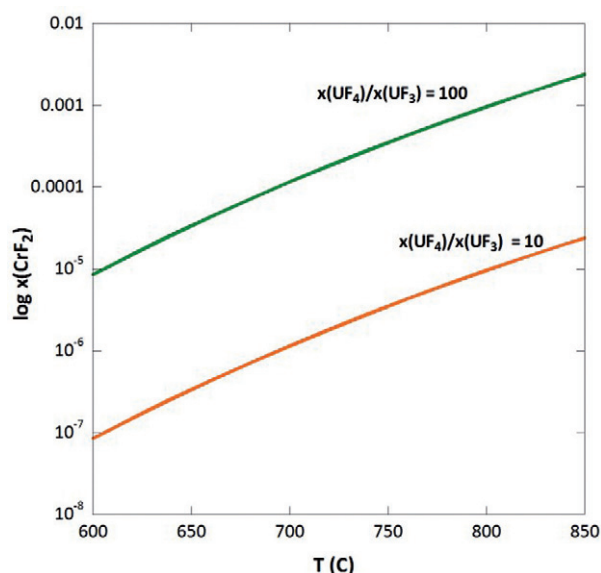


Fig. 3 Variation of the logarithm of the mole fraction of CrF_2 in the fuel salt as a function of temperature for various ratios $x(\text{UF}_4)/x(\text{UF}_3)$.

Table 2 Equilibrium constants of dissolution for Cr, Fe and Ni at several temperatures

Dissolution reaction: $\text{M} + 2\text{UF}_4 = 2\text{UF}_3 + \text{MF}_2$

$$K_N(\text{M}) = \frac{x(\text{MF}_2)x(\text{UF}_3)^2}{x(\text{M})x(\text{UF}_4)^2}$$

| T (C) | Cr | Fe | Ni |
|-------|-----------------------|------------------------|-----------------------|
| 800 | $4.644 \cdot 10^{-7}$ | $1.075 \cdot 10^{-10}$ | |
| 727 | $2.8 \cdot 10^{-7}$ | $4.55 \cdot 10^{-10}$ | |
| 700 | $1.527 \cdot 10^{-7}$ | $2.16 \cdot 10^{-10}$ | $1.67 \cdot 10^{-17}$ |
| 600 | $1.172 \cdot 10^{-7}$ | $1.08 \cdot 10^{-10}$ | $9.38 \cdot 10^{-18}$ |

dissolved CrF_2 as a function of temperature is the driving force for the mass transfer experimentally⁶¹ observed from hot areas to cold areas in thermal convection loops. Dissolution of chromium occurs in hot parts. And the formed CrF_2 may be reduced in colder sections. The dissolution of chromium as calculated from Eq. 11 should be negligible for the lower salt potential values (U ratio equals to 10).

It was observed that the redox potential, diffusion coefficients, salt composition hydraulic conditions and operating time all influence the mass transfer process.

Values of K_N derived from Grimes' experimental results⁶³ for nickel, chromium and iron at different temperatures are given in Table 2. Their analysis indicates that nickel is chemically stable in most fluoride salt and is not affected by oxidation. The constants for iron range between those of chromium and nickel. Therefore, iron could be affected by oxidation under uncontrolled redox conditions. This supports a well known experimental observation: Ni-based alloys are more appropriate from a chemical point of view for use in MSR systems than stainless steels.

Thermodynamical approach to the corrosion

Most of the experimental results^{65,66} and observations can be understood by a thermodynamical approach based on data from pure compounds. Thermodynamical diagrams that give the stability domains of elements under their different forms as a function of potential and oxoacidity (related to the oxide concentration in the salt) have been calculated in fluoride molten salts for the main elements of the structural alloys, Ni, Fe, Cr, Mo and W (Fig. 4). The calculation procedure, using the thermodynamical data of pure compounds⁵² has been described previously⁶⁷. In this paper the approach is described for pure metals. In the case of alloys, the calculations have to be corrected using the activities of each constituent element of the alloy (the activity can be assumed to be equal to the mole fraction for very dilute solutions or in cases where the activity coefficients are unknown). The fluoroacidity of the molten salt, which is given by the amount of free fluoride ions in the salt, has a large influence on the speciation of oxides and metallic fluorides. The fluoroacidity depends on the fluoride salt composition. For instance, in the case of FLiNaK, the fluoride activity is assumed to be equal to 1 because the salt is totally dissociated and

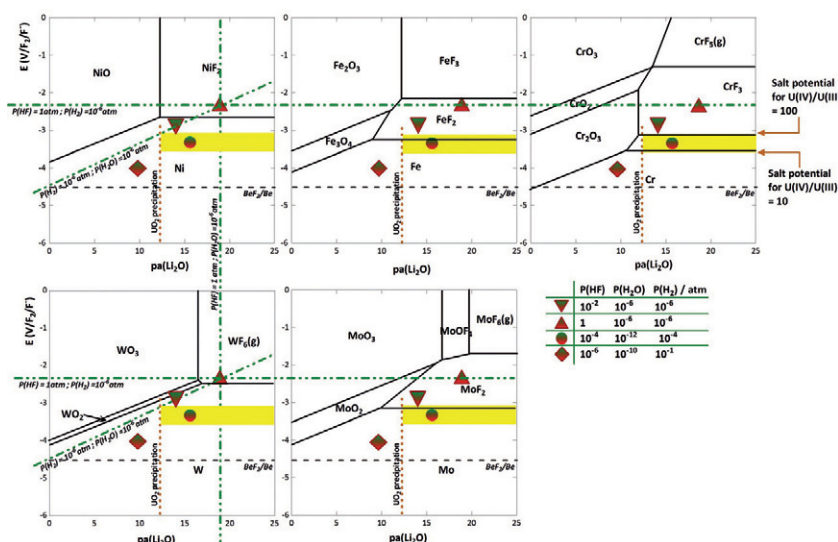


Fig. 4 Potential-acidity diagrams calculated at 700°C for Ni, Fe, Cr, W and Mo in FLiBe fluoride salt ($a(\text{LiF}) = 0.66$). ($pa(\text{Li}_2\text{O}) = -\log(a(\text{Li}_2\text{O}))$). The equations used for the calculation of gas mixtures (green curves and red symbols) are:

$$pa(\text{Li}_2\text{O}) = \log K_{(\text{H}_2\text{O}/\text{HF})} - 2\log a(\text{LiF}) - \log P(\text{H}_2\text{O}) + 2\log P(\text{HF}) \quad (\text{from Eq. 13}); \quad E_{(\text{HF}/\text{H}_2)} = E^\circ + (2.3RT/2F) \log(P(\text{HF})^2/P(\text{H}_2)) \quad (\text{from Eq. 14});$$

$$E_{\text{H}_2\text{O}/\text{H}_2} = E^\circ + (2.3RT/2F) \log(P(\text{H}_2\text{O})a(\text{LiF})^2/P(\text{H}_2)) + 2.3RT/2F pa(\text{Li}_2\text{O}) \quad (\text{from Eq. 15}).$$

The yellow domain is calculated from Eq. 3 for $\text{U(IV)}/\text{U(III)}$ ratios varying between 10 and 100."

the salt is (fluoro)basic. In the case of $\text{LiF}-\text{BeF}_2$, BeF_2 is a (fluoro)acid salt which forms complexes with fluorides. Therefore, the amount of free fluoride ions depends on the LiF/BeF_2 ratio. In the case of $\text{LiF}-\text{BeF}_2$ (66-34 mol%) the activity of free fluoride ions is very low, the metal speciation is low and the activity coefficient of the metals are close to unity⁷⁹. Therefore, the speciation of the metallic fluoride depends on the molten salt fluoroacidity, the redox potential MF_x/M depends on the speciation and thus the chemical behavior of the metals depends on the salt composition. The activity coefficients of metallic fluorides are not known for all molten salts and all compositions. Therefore this preliminary thermodynamical approach does not consider the metal activities, and is a more global approach to the chemical behavior of metals in molten salts. The exact data can easily be calculated by knowing the activity coefficients of the metallic fluorides in a given fluoride molten salt.

Nevertheless, diagrams in Fig. 4 considering pure metals give a global appreciation of the metal stability in a fluoride environment

Low potential values (bottom of the Y scale) correspond to the stability domains of the metallic compounds (oxidation state of zero). The oxoacidity of the salt is equivalent to the oxide content and this data is calculated by considering the activity of Li_2O ⁶⁷. High values of $pa(\text{Li}_2\text{O})$ (right side of X scale) correspond to high oxoacidities (low oxide concentrations). The diagrams are colored to show the influence of the molten salt chemistry and the influence of the gas mixture introduced into the molten salt. The potential domain of the salt controlled by the ratio UF_4/UF_3 is colored yellow. Let's assume this ratio can vary from 10 to 100. UF_3 is known to disproportionate to

UF_4 and U. Experimental measurements have demonstrated⁶³ that this reaction has no influence on the salt chemistry as the ratio UF_4/UF_3 remains above 10. The highest value (100) is the limit for an acceptable corrosion⁶³. Combining the phase diagrams for the metals and the potential range of the salt indicates that nickel and tungsten cannot be oxidized under usual salt application conditions, iron and molybdenum can be oxidized under the highest oxidizing conditions and under most potentials, and chromium is not stable but oxidizes to CrF_2 or CrF_3 .

In Fig. 4, the colored symbols indicate the potential/acidity set by a given gaseous mixture. These were found by considering the following equations:



A mixture of two gasses forms a straight line (vertical, horizontal or oblique) (green lines in Fig. 4). A mixture of three gasses gives a single point; both potential and acidity are fixed. This shows that a strict control of the chemical conditions in the salt, and thus of the reactions between salt and metals, can only be achieved through use of three gasses (the composition is given by the red points in Fig. 4).

A high HF pressure helps increase the potential and the oxoacidity: less oxide but highly oxidative conditions. As it was already experimentally observed, stability diagrams show that purification by pure HF may lead to metal oxidation.

As can be observed in the calculated diagrams, the potential can be controlled in two ways. The first way is using a reductant to manage a

soluble/soluble redox system as is proposed in the case of the molten salt reactor: the use of metallic Be^{22-28,43,47} is recommended for MSRE and MSBR concepts and also in fusion concepts to reduce impurities or fission products produced during the neutronic reactions. In the case of MSFR concept, metallic Th is recommended³⁸. The second way is the gas mixture: as it is shown on the diagrams, a given gas composition fixes the redox potential and the oxoacidity of the salt. To control the salt potential in AHTR systems, a gas mixture could be envisaged.

Corrosion prevention

Material coatings have been proposed to prevent corrosion of structural materials⁴². These protecting layers can be realized by chemical^{68,69} or electrochemical processes. Electrodeposition in molten salts is recommended for refractory metals (Nb, Ta)⁷⁰⁻⁷³. Nevertheless, the coating requirements are adherence, homogeneity and good coverage to bring a strong protection to structural material. Only small fissures could induce corrosion of the main material.

Salt chemistry also has to comply with given specifications (especially in terms of solubility for fissile elements and fission products), but control of the oxidation potential of the salt seems to be achievable. It is a challenge to measure the melt potential within molten fluoride salts, and hence to be able to anticipate an increase of the redox potential. Reference electrodes have been proposed, generally based on the reference redox system, NiF_2/Ni ^{74,75}. Russian researchers have developed an innovated system using a dynamic reference electrode⁷⁶.

A unique method to protect the structural material was investigated in the 1980s. The device or facility walls were cooled down to allow for the formation of a frozen salt layer on the wall surface. The dissolution reactions are then strongly decreased. Corrosion tests performed in FLiBe have shown that the method results in a corrosion rate of lower than $0.5 \mu\text{m}/\text{year}$ ^{41,77,78}. However, this technique is not feasible for an energy conversion system.

Corrosion investigation techniques

The corrosion is often investigated by specimen immersion for various times in various conditions and analyzed afterward. Some electrochemical techniques have been developed to study the corrosion *in-situ* such as the impedance spectroscopy or the Tafel evolution analysis. The difficulty associated with these methods is that it is necessary to apply a potential to the metallic specimen and therefore to induce a corrosion via an electrochemical process.

An innovative technique such as Scanning Electrochemical Microscopy is under development by our team to describe the corrosion mechanism of metallic alloys in a molten salt in controlled conditions of potential, oxoacidity and atmosphere. The technique is based on the use of a microprobe electrode (Fig. 5) which is introduced into the diffusion layer of the metallic specimen in contact with the melt. The electrochemical measurements allow analysis of the

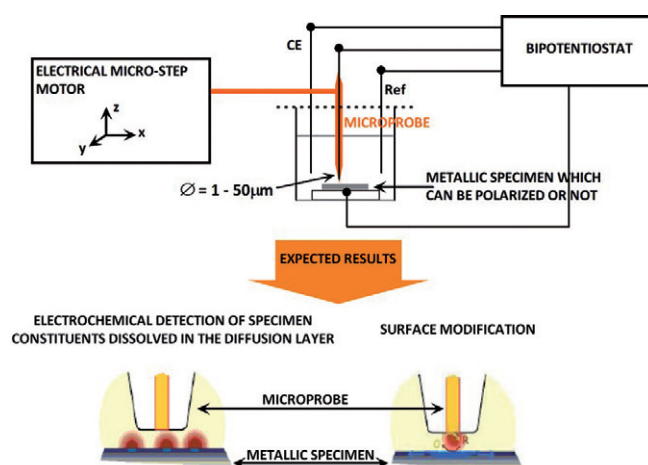


Fig. 5 Scheme for the scanning electrochemical microscopy technique and results expected for corrosion investigations.

elements dissolved in the diffusion layer at very low concentrations. This technique also enables the observation of the surface of the specimen and especially the formation of passivating layers. This method has two main advantages:

- There are no direct electrochemical measurements of the specimen (no forced oxidation).
- This method is an *in-situ* method. Therefore it is possible to modify one experimental parameter and directly and immediately observe its effect on the corrosion mechanism.


Even if this method has already been applied for corrosion studies in aqueous solution^{80,81}, its development for corrosion investigations in molten salt media is a major technical challenge.

Conclusion

Thermodynamical calculations based on pure compounds can help to understand some of the reactions involved in the corrosion of structural materials in MSR systems and other applications. The dissolution of metallic elements is due to oxidative processes in the molten salt which contains oxidizing impurities and/or uranium fluoride. Corrosion may be mitigated by both selecting an appropriate material and controlling the salt chemistry. However, it is important to bear in mind that the choice of a structural material is not solely driven by its environmental compatibility, and that other properties have to be considered, such as the mechanical properties at high temperature, resistance under irradiation, forming ability, etc.

One issue regarding corrosion in nuclear applications using molten salts, and particularly molten salt nuclear reactors, is the evolution of the salt composition during operation: production of HF (by an uncontrolled purification process, hydrolysis reactions or water trace dissolution), production of highly corrosive fluorine and corrosive fission products (by fission reaction), and mass transfer (dissolution/

deposition structural material processes) due to in-reactor's thermal gradients. The interface material/salt cannot be considered as a static interface, but must be recognized as dynamic, and so the kinetics of

the interfacial processes must be carefully investigated. This should help provide specifications for an internal and continuous control of the redox potential to mitigate corrosion. 

REFERENCES

- Delons, L., et al., *Procédé de séparation des tétrachlorures de zirconium et d'hafnium*, Patent n°0105265, 2001.
- Groult, H., *J Fluorine Chem* (2003) **113**, 173.
- Griffiths, T. R., et al., *J Alloy Compd* (2006) **418**, 116.
- Moriyama, H., et al., *J Alloy Compd* (1998) **271-273**, 587.
- Ackerman, J. P., *Prog Nucl Energ* (1997) **31**, 141.
- Lacquement, J., et al., *J Fluorine Chem* (2009) **130**, 18.
- Delpach, S., *Electrochemical and molten salt liquid-metal extraction for nuclear applications*, Proceeding of the SESTEC 2008 conference, Delhi, 2008.
- Cassayre, L., et al., *J Nucl Mater* (2007) **360**, 49.
- Takeuchi, M. et al., *J Phys Chem Sol* (2005) **66**, 521.
- Kenisarin, M. M., *Renew Sust Energ Rev* (2010) **14**, 955.
- Forsberg, C. W., et al., *J Sol Energ Eng* (2007) **129**, 141.
- Haubenreich, P. N., and Engel, J. R., *Nucl Appl Techn* (1970) **8**, 118.
- Grimes, W. R., *Nucl Appl & Techn* (1970) **8**, 137.
- Bettis, E. S., and Robertson, R. C., *Nucl Appl Techn* (1970) **8**, 190.
- Uhler, J., *J Nucl Mater* (2007) **360**, 6.
- Hosnedl, P., et al., *Review of Molten Salt Reactor Technology: review and analysis of the structural material*, MOST European report, 2003.
- Moriyama, H., et al., *Fusion Eng Des* (1998) **39-40**, 627.
- Moir, R. W., *Fusion Eng Des* (1995) **29**, 34.
- Nygren, R. E., et al., *Fusion Eng Des* (2004) **72**, 181.
- Nagasaka, T., et al., *J Nucl Mater* (2009) **386-388**, 716.
- Nagasaka, T., et al., *Fusion Eng Des*, in press (2010).
- Cheng, E. T., et al., *Fusion Eng Des* (2003) **69**, 205.
- Petti, D. A., et al., *Fusion Eng Des* (2006) **81**, 1439.
- Keiser, J. R., et al., *J Nucl Mater* (1979) **85-86**, 295.
- Kondo, M., et al., *J Nucl Mater* (2009) **386**, 685.
- Simpson, M. F., et al., *Fusion Eng Des* (2006) **81**, 541.
- Nishimura, H., et al., *Fusion Eng Des* (2001) **58-59**, 667.
- Calderoni, P., et al., *J Nucl Mater* (2009) **386-388**, 1102.
- Nishimura, H., et al., *J Nucl Mater* (2002) **307-311**, 1355.
- Kondo, M., et al., *Fusion Eng Des* (2009) **84**, 1081.
- Ambrosek, J., et al., *Nucl Techn* (2009) **165**, 166.
- Peterson, P. F., and Zhao, H., *A flexible baseline design for the advanced high temperature reactor using metallic internals (AHTR-MI)*, Proceedings of ICAPP'06 Reno, USA, paper 6052, 2006.
- Olson, L. C., et al., *J Fluorine Chem* (2009) **130**, 67.
- Delpach, S., et al., *J Fluorine Chem* (2009) **130**, 11.
- Merle-Lucotte, E., et al., *Optimizing the burning efficiency and the deployment capacities of the molten salt fast reactor*, Proceedings of Global 2009, Paris, France, paper 9149, (2009).
- LeBlanc, D., *Nuclear Engineering and design* (2010) **240**, 1644.
- LeBrun, C., *J Nucl Mater* (2007) **360**, 1.
- Delpach, S., et al., *MSFR: Material issues and the effect of chemistry control*, Proceeding of the GIF symposium, Paris, France, (2009) 201.
- Blood, C. M., Solubility of NiF₂ in LiF-Bef₂ (61-39 mol%), ORNL-2551, pp 93, 1985.
- McCoy, H. E., Jr, *Status material development for molten salt reactions*, ORNL/TM-5920, 1978.
- Broc, M., et al., *J Nucl Mater* (1983) **119**, 123.
- Santarini, G., *J Nucl Mater* (1981) **99**, 269.
- Taboada, A., *Molten salt reactor program, Metallurgical developments*, ORNL report, ORNL-3708 pp331, 1964.
- McCoy, H. E., *Influence of Ti, Zr and Hf additions on the resistance of modified Hastelloy N to irradiation damage at high temperature*, ORNL report, ORNL-TM3064, 1971.
- McCoy, H. E. and Sessions, C. E., *Molten salt reactor program, Materials developments*, ORNL-4676, 1971.
- CEA-EDF, *Filière "Sels Fondus", Dossier technique*, CEA/DCH/DGR/ADJT/76-51 ; EDF/HT-13/11/76, 1976.
- Cabet, C., *Tenue à la corrosion des matériaux métalliques dans les réacteurs à sels fondus*, Rapport technique CEA, RT-SCCME 558, 2001.
- Metzger, G. E., *Nucl Eng & Des* (1968) **7**, 29.
- McCoy, H. E. and Gehlbach, R. E., *J Nucl Mater* (1971) **40**, 151.
- Cury, R., et al., *Intermetallics* (2009) **17**, 174.
- Chang, T., and Lansing, F., *Review of corrosion causes and corrosion control in a technical facility*, NASA Technical Reports, TDA Progress Report, pp 145, 1982.
- Barin, I. et al., *Thermodynamic Properties of Inorganic Substances*, Springer Verlag, Berlin, 1977.
- Cartier, R., *Propriétés électrochimiques de l'uranium, du cérium et du zirconium dans l'eutectique LiF-BaF₂*, CEA, Report CEA-R-3792, 1969.
- Grimes, W. R., and Guner, D. G., *Molten salts as reactor fuel*, *Reactor Handbook*, Interscience Publishers, New York, 1960.
- Field, P. E., and Shaffer, J. H., *J Phys Chem* (1967) **71**, 3218.
- Shaffer, J. H., et al., *J Phys Chem*, (1959) **63**, 1999.
- Pizzini, S., and Morlotti, R., *Electrochim Acta* (1965) **10**, 1033.
- Manning, D. L., *J Electroanal Chem* (1963) **6**, 227.
- Keiser, J. R., *Status of tellurium-Hastelloy N studies in molten fluoride salts*, ORNL/TM-6002, 1977.
- Fabre, S., et al., *J Nucl Mater*, submitted.
- Koger, J. W., *Effect of FeF₂ addition on mass transfer in a hastelloy N-LiF-Bef₂-UF₄ thermal convection loop system*, ORNL/TM-4188, 1972.
- Koger, J. W., ORNL/TM-3866, pp21, 1972.
- Grimes, W. R., ORNL-3708, pp 238, 1964.
- Baes, C. F., *Proc Nuclear Fuel*, Conf. 690801 USAEC, 1969.
- Pourbaix, M., *Corrosion Science* (1990) **30**, 963.
- Olander, D., *J Nucl Mater* (2002) **300**, 270.
- Rouquette-Sanchez, S., and Picard, G. S., *J Electroanal Chem* (2004) **572**, 173.
- Koger, J. W., et al., US Patent Office n°3783014, 1974.
- Jeong, S. M., et al., *J of Alloys and Compounds* (2008) **452**, 27.
- Broc, M., et al., *Plating of refractory metals by electrolysis in molten salts*, *Molten salt electrolysis in Metal production*, Intern. Symp. The Institution of Mining and Metallurgy, Grenoble, France, 1977.
- Travalloni, A., *Dépot électrolytique de Nb à partir de fluorures fondus*, Thesis UPMC, Paris, France, 1978.
- Taxil, P., and Mahenc, J., *Corros Sci* (1981) **21**, 31.
- Cardarelli, F., et al., *Int J Refract Met H* (1996) **14**, 365.
- Jenkins, H. W., et al., *Electroanal Chem Interfacial Electrochem* (1968) **19**, 385.
- Winand, R., and Chaudron, G., *Compt Rend* (1967) **264C**, 649.
- Afonichkin, V. K., et al., *J Fluorine Chem* (2009) **130**, 83.
- E. D. F., *Brevet FR 2299702*, 1974.
- E. D. F. and P. U. K., *Brevet FR 2314558*, 1975.
- Baes, C. F., Jr, *J Nucl Mater* (1974) **51**, 149.
- Yin, Y., et al., *Appl Surf Sci* (2009) **255**, 9193.
- Völker, E., et al., *Electrochem Comm* (2006) **8**, 179.